

ARTICLE

Kinetics of Photogenerated Electrons Involved in Photocatalytic Reaction of Methanol on Pt/TiO₂[†]

Tao Chen, Guo-peng Wu, Zhao-chi Feng, Jian-ying Shi, Gui-jun Ma, Pin-liang Ying, Can Li*

State Key Laboratory of Catalysis, Dalian Institute of Chemical Physics, Chinese Academy of Sciences, Dalian 116023, China

(Dated: Received on May 22, 2007; Accepted on July 10, 2007)

Time-resolved IR spectroscopy was used to detect the photocatalytic reaction of methanol for H₂ production on Pt/TiO₂ catalysts. There exists an optimal amount of Pt loading in the Pt/TiO₂ catalysts for the reaction of the photogenerated long-lived electrons. For a given amount of Pt loading, the reaction rate of the long-lived electrons on Pt/TiO₂ catalysts varies greatly with the different reduction temperature of the catalysts. The possible reason is that the Pt particles occupy the surface active sites for methanol adsorption on Pt/TiO₂ catalysts reduced at high temperature. This phenomenon is not observed obviously on Pt/TiO₂ catalysts reduced at low temperature. The decay rate of the long-lived electrons evaluated by time-resolved IR method qualitatively correlates well with the activity of H₂ production under steady-state irradiation conditions.

Key words: Methanol photocatalytic reaction, Time-resolved IR, Pt/TiO₂ photocatalyst, Photogenerated electron, Decay kinetic

I. INTRODUCTION

The photocatalysis on TiO₂ has attracted considerable attentions because of the excellent properties of TiO₂ and TiO₂ based photocatalysts in degradation of environmental pollutants [1,2], H₂ generation from water or organic compounds [3-5], solar-to-electric energy conversion [6,7], and so on. To understand the mechanisms of these photoassisted or photocatalytic processes, photocatalytic production of H₂ from methanol is one of the most suitable model reactions because this photocatalytic reaction proceeds with high efficiency and methanol is a simple and important organic compound with one reactive functional group. In addition, this reaction is carried out under anaerobic conditions, which avoids considering the function of O₂. If the mechanisms of this fundamental photocatalytic reaction are not well understood, it may be difficult to make clear the mechanisms of more complex systems.

Time-resolved absorption spectroscopy has been developed to study kinetics of the photogenerated charge carriers in semiconductor catalysts [8-11]. It was found that the absorption in mid-IR region is due to the free and/or trapped electrons [12-16]. Because there is no interference of the holes in mid-IR region, and the shape of the mid-IR absorption spectra is not sensitive to surrounding conditions, time-resolved mid-IR absorption spectroscopy is potentially a powerful tool to accurately trace the kinetics of the electrons. Re-

cently, Yamakata *et al.* utilized a home-made mid-IR absorption spectroscopy with nanosecond to second time resolution to study the photocatalytic reaction of methanol on Pt/TiO₂ and observed that the amount of long-lived electrons in platinized TiO₂ increases significantly after 50 ns [17,18]. They proposed that adsorbed methoxy groups captured the holes within 50 ns, which has been demonstrated by a recent femtosecond time-resolved UV-Visible spectroscopy study, in which the authors directly observed that most of the holes were captured by adsorbed methanol within 1 ns [19]. We previously reported that the long-lived electrons in this reaction system are important for H₂ generation and the electron decays on millisecond to second time scale in Pt/TiO₂ corresponds to the electron consumption for H₂ evolution [20]. It was also found that, for the Pt/TiO₂ catalysts reduced in H₂ at 400 °C, there existed an optimal amount of Pt loading for the reaction rate of the long-lived electrons [20].

In this work, time-resolved IR spectroscopy was used to study the kinetics of the long-lived electrons in the photoreaction of methanol on Pt/TiO₂ catalysts for H₂ generation. The effects of Pt loading amount and reducing temperature of Pt/TiO₂ catalysts on the reaction rate of the long-lived electrons were studied in detail. The correlation between the kinetics of the long-lived electrons and the activity of H₂ production under steady-state UV irradiation conditions was also investigated to further understand the mechanisms of this photocatalytic reaction.

II. EXPERIMENTS

A. Sample preparation and characterization

Pt loaded TiO₂ catalysts, Pt/TiO₂, were prepared by impregnation method. The commercially available

[†]Part of the special issue "Cun-hao Zhang Festschrift".

*Author to whom correspondence should be addressed. E-mail: canli@dicp.ac.cn, Tel.: +86-411-84379070, Fax: +86-411-84694447

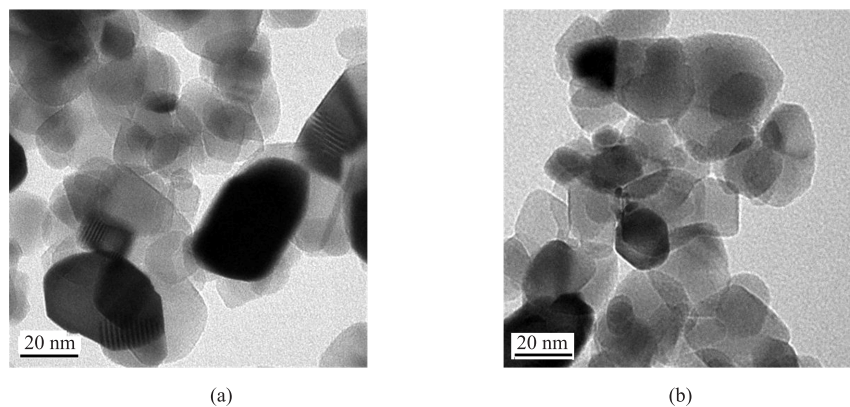


FIG. 1 Transmission electron micrographs of the Pt/TiO₂ catalysts. (a) Pt/TiO₂-200 (1.0 wt%); (b) Pt/TiO₂-400 (1.0 wt%).

TiO₂, generally known as Degussa P25 (20% rutile, 80% anatase), was used as the support. Briefly, 1 g P25 was dispersed into 30 mL H₂PtCl₆ aqueous solution at a given concentration and stirred for 6 h. After evaporation to dryness at 373 K, the obtained dry powder was then reduced with H₂ at 200 or 400 °C for 2 h. The final products are designated as Pt/TiO₂-*T* (*n* wt%), where *T* represents the reducing temperature and *n* represents the value of weight percentage of Pt.

The transmission electron micrographs (TEM) were obtained with Tecnai G² F30 microscope. In the measurements, the samples were suspended in ethanol and mounted on a plastic film supported on a Cu grid. The energy dispersion X-ray (EDX) analysis was also carried out accompanying with the TEM studies.

B. Time-resolved IR measurement

The transient IR absorption signals were recorded on a Nicolet 870 FTIR spectrometer and the detail experimental methods were reported elsewhere [20]. Briefly, the Pt/TiO₂ sample was pressed into a self-supporting wafer (about 20 mg) and put into a quartz IR cell with BaF₂ windows. The IR cell was connected to the vacuum system. Before each run of the experiment, the sample in the cell was heated to 573 K under vacuum (0.13 Pa) for 1 h. After the heating, when the sample was cooled to room temperature under the protection of N₂ atmosphere, the IR cell with the sample was evacuated and the methanol vapor was then introduced. The transient IR absorption spectra were measured by step-scan measurement mode. The laser at 355 nm with 10 ns pulse width from third harmonic generation of a Q-switched Nd: YAG laser (Labeit Beijing) was used as the excitation source. To observe the slow decaying signals ranging from millisecond to second, the stepping mirror was stopped to one fixed position and the 20 MHz DC output of the MCT amplified by AC-coupled SR560 preamplifier (1 MHz-0.03 Hz) was used to measure the transient signals ($\Delta I'(t)$).

The laser induced transient signals were accumulated and averaged in the external oscilloscope (Tektronix, TDS5104). From the knowledge of circuit analysis, the recorded transient signals ($\Delta I'(t)$) is the convolution of $\Delta I(t')$ and $g(t)$:

$$\Delta I'(t) = \int_{-\infty}^{\infty} \Delta I(t')g(t-t')dt'$$

where $g(t)$ represents the unit-impulse response of the whole electronic systems and $\Delta I(t)$ represents the undistorted curve. $g(t)$ was determined experimentally. Through the deconvolution, the true transient curve $\Delta I(t)$ was obtained. Before measuring the transient signals, the DC output of MCT modulated by a hand-made chopper was used to measure the intensity of the whole IR light in 1000-4000 cm⁻¹ (*I*) and the average transient absorbance changes were calculated as

$$\Delta A(t) = -\lg \left\{ \frac{1}{I} \left[I + \frac{\Delta I(t)}{g} \right] \right\}$$

where *g* is the gain of the AC-coupled preamplifier.

C. Photocatalytic activity

The photocatalytic H₂ production under steady state irradiation conditions was investigated in a pyrex reaction cell connected to a closed gas circulation and evacuation system [21]. The light source was a 300 W Xe lamp with a water-cooled quartz jacket. 0.3 g catalyst was suspended in an aqueous solution containing 160 mL H₂O and 40 mL CH₃OH. Before the experiment, the reaction mixture was deaerated thoroughly. The evolved H₂ was measured by online gas chromatography.

III. RESULTS AND DISCUSSION

The particle sizes of Pt on the catalysts were studied by TEM measurements. Figure 1 shows the transmission electron micrographs of Pt/TiO₂-200 (1.0 wt%)

and Pt/TiO₂-400 (1.0 wt%) catalysts. It can be seen that the surface of the TiO₂ particles is very clean and no Pt particles can be seen clearly. The results indicate that the particle sizes of Pt are too small to be seen (usually smaller than 1 nm) from transmission electron micrographs. The EDX analysis was carried out at several different places (50 nm×50 nm) on the catalysts. The results (not shown) indicate that the distribution of Pt on the prepared catalysts is very uniform.

Figure 2 shows the three-dimensional time-resolved IR absorption spectra of Pt/TiO₂-200 (0.2 wt%) in vacuum recorded by step scan measurement mode after laser excitation. A broad UV-induced IR absorption appears and the absorption monotonously increases in intensity with lower wavenumbers. The broad and structureless IR absorption is assigned to intraband transitions of CB electrons or excitation of shallowly trapped electrons to the CB [12-16,22,23]. The broad IR absorption spectrum obeys the equation:

$$\Delta\text{Absorbance} = A\tilde{\nu}^{-p}$$

where $\tilde{\nu}$ is the wavenumber, A is a constant, and p is the scattering constant [12-16]. Fitting the spectrum data into above relation, p was determined as about 1.7, close to the ideal value of 1.5 when the absorption of the photons is associated with scattering of the acoustic phonons. Zhao *et al.* reported that free conduction-band electrons are tightly coupled with the acoustic lattice phonons to conserve the momentum during the intraband transitions [16]. So it is deduced that the electrons giving above broad IR absorption are mainly the free CB electrons. The photogenerated electrons mainly decay on microsecond time scale as shown in Fig.2. When the sample exposed to methanol was measured, the shape of the absorption spectra does not change but the intensity of the absorbance strongly increases (not shown). The photogenerated electrons in Pt/TiO₂ decay extremely slowly in the presence of methanol.

Figure 3 shows the normalized IR absorption decay curves of Pt/TiO₂-200 with different loading amount

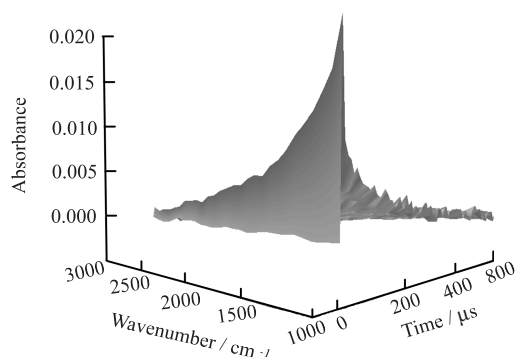
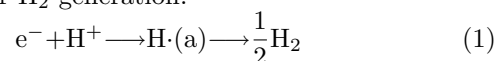


FIG. 2 Time-resolved IR absorption spectrum of Pt/TiO₂-200 (0.2 wt%) in vacuum recorded by step scan measurement mode. 3 Hz, 8 mJ/pulse 355 nm laser was used to excite the sample.

of platinum. The pressure of methanol was fixed to 2.7 kPa. In our previous paper [20], it was reported that the electron decays on millisecond to second time scale in Pt/TiO₂ are mainly due to the electron consuming reaction for H₂ generation:



This reaction is catalyzed by Pt particles. The shape of the decay curves is insensitive to the UV pulse energy in the range of 2-6 mJ, which suggests that the decays of the long-lived electrons apparently obey the exponential decay kinetics. The decay curves can be fitted well by the two-exponential formula:

$$y = A_1 \exp\left(-\frac{x}{\tau_1}\right) + A_2 \exp\left(-\frac{x}{\tau_2}\right)$$

The single-exponential or multi-exponential decay kinetics was successfully used to analyze some charge recombination processes that are quite different from the slow decay process of the long-lived electrons observed in our experiments [13,24,25]. Because not all the electrons are consumed in the interval of laser pulses (10 s) and a small amount of electrons might be accumulated in the catalysts, the curves are fitted by the adjusted formula,

$$y = A_1 \exp\left(-\frac{x}{\tau_1}\right) + A_2 \exp\left(-\frac{x}{\tau_2}\right) - A_1 \exp\left(-\frac{10}{\tau_1}\right) - A_2 \exp\left(-\frac{10}{\tau_2}\right)$$

The lifetime and relative amplitudes from the non-linear least-squares fits are listed in Table I. Figure 4 shows the dependence of the simulated rate constants of the fast component on the Pt loading amount. It can be seen that there exists an optimal amount of Pt loading for reaction (1) and the maximum rate was obtained with 0.1 wt%Pt loaded TiO₂. With further increase of Pt loading amount, the rate declines. These

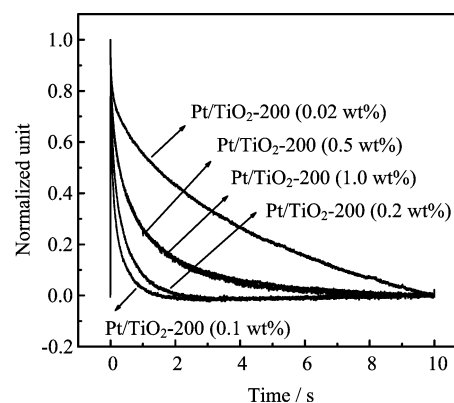


FIG. 3 Normalized transient profiles of average IR absorption of Pt/TiO₂-200 samples excited by 355 nm laser pulse of 10 ns duration. The decay curves were recorded at RT by accumulating 50 traces repeated at 0.1 Hz when the pre-treated samples were exposed to ~2.7 kPa CH₃OH.

TABLE I The lifetime and relative amplitudes from two exponential fits of the decay curves

Sample	$A_1/\%$	τ_1/s	$A_2/\%$	τ_2/s
Pt/TiO ₂ -200 (0.02 wt%)	19	0.39	81	6.57
Pt/TiO ₂ -200 (0.1 wt%)	51	0.042	49	0.35
Pt/TiO ₂ -200 (0.2 wt%)	39	0.057	61	0.51
Pt/TiO ₂ -200 (0.5 wt%)	56	0.29	44	2.30
Pt/TiO ₂ -200 (1.0 wt%)	46	0.26	54	1.83

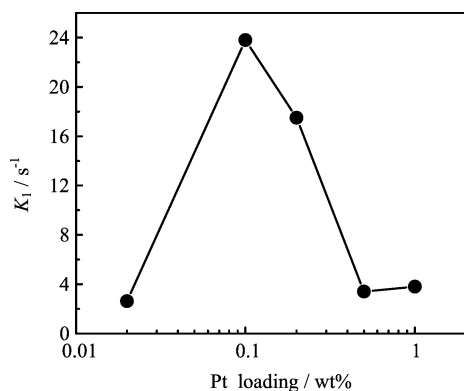


FIG. 4 Dependence of the simulated rate constants of the fast component on Pt loading amount for Pt/TiO₂-200 catalysts.

results indicate that a small amount of Pt loading is effective enough to catalyze reaction (1). Further increasing Pt loading amount increases the reactive sites for reaction (1), but both of the concentration of the electrons trapped by each Pt particle and the probability of the protons that can arrive at one Pt particle decrease. It is a possible reason to explain why the rate of reaction (1) decreases with excessively increasing Pt loading amount.

The regularities for Pt/TiO₂ samples reduced in H₂ at 200 °C shown in Fig.4 are similar to the previously published results for Pt/TiO₂ catalysts reduced in H₂ at 400 °C [20], but it is worthy to note that the decay kinetics of the long-lived electrons in the Pt/TiO₂-200 samples is different from that in Pt/TiO₂-400 sample. Figure 5 shows the normalized transient profiles of average IR absorption of Pt/TiO₂-200 (0.1 wt%) and Pt/TiO₂-400 (0.1 wt%) samples excited by 355 nm laser pulse of 10 ns duration. Figure 6 shows the normalized transient profiles of average IR absorption of Pt/TiO₂-200 (1.0 wt%) and Pt/TiO₂-400 (1.0 wt%) samples excited by 355 nm laser pulse of 10 ns duration. Above results indicate that the long-lived electrons in Pt/TiO₂-200 (0.1-1.0 wt%) catalysts decay faster than those in Pt/TiO₂-400 (0.1-1.0 wt%) catalysts when the Pt loading amount is the same. Figure 7 shows the FTIR spectra taken after the adsorption of CH₃OH on Pt/TiO₂-200 catalysts and then evacuation at room temperature. The spectra of the catalysts recorded in vacuum are

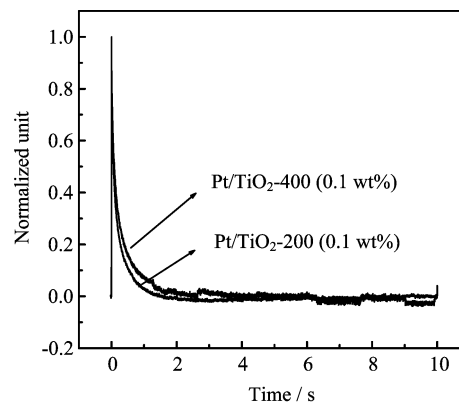


FIG. 5 Normalized transient profiles of average IR absorption of Pt/TiO₂ (0.1 wt%) samples excited by 355 nm laser pulse of 10 ns duration. The decay curves were recorded at RT by accumulating 50 traces repeated at 0.1 Hz when the pretreated samples were exposed to ~2.7 kPa CH₃OH.

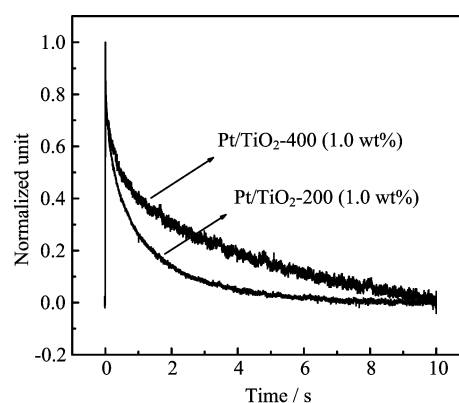


FIG. 6 Normalized transient profiles of average IR absorption of Pt/TiO₂ (1.0 wt%) samples excited by 355 nm laser pulse of 10 ns duration. The decay curves were recorded at RT by accumulating 50 traces repeated at 0.1 Hz when the pretreated samples were exposed to ~2.7 kPa CH₃OH.

subtracted. It is observed that undissociated adsorbate CH₃OH and dissociated adsorbate CH₃O are formed on the catalyst surface, with the characteristic frequencies of symmetric and antisymmetric CH₃ stretching at 2843 and 2944 cm⁻¹ for CH₃OH, 2818 and 2923 cm⁻¹ for CH₃O [26,27]. As shown in Fig.7, the IR absorbance of CH₃OH and CH₃O on Pt/TiO₂-200 catalysts almost do not decrease with increasing Pt loading amount, but when Pt/TiO₂-400 catalysts were measured, the capacity of methanol adsorption decreases strongly with the increase of the Pt loading [20].

Scheme 1 shows the proposed model representing the different interactions between the metal and the supporter in Pt/TiO₂ catalysts reduced in H₂ at 200 and 400 °C. It has been reported that the strong metal-support interaction (SMSI) effect occurs when the noble metal loaded TiO₂ catalysts are reduced in H₂ at high temperature (usually >300 °C) [28]. The strong

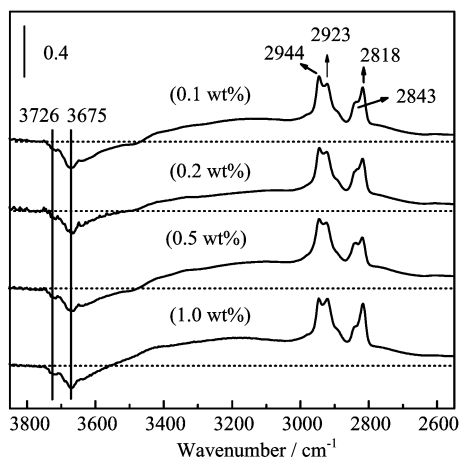
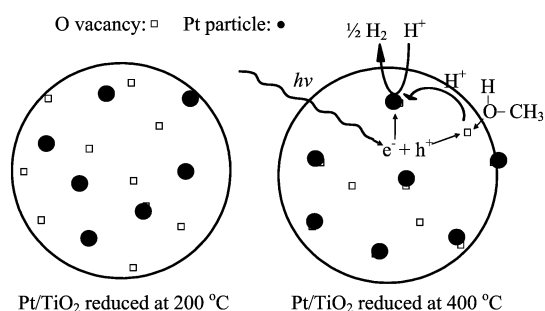


FIG. 7 FTIR spectra of adsorbed CH₃OH on Pt/TiO₂-200 samples at RT. The subtracted spectra of the catalysts exposed to about 267 Pa CH₃OH vapor followed by evacuation for 15 min are shown.



Scheme 1: The proposed model representing the different metal-support interactions in Pt/TiO₂.

interaction of Pt-Ti³⁺ [29] leads to the decrease of Ti³⁺ sites (oxygen vacancy sites) for methanol adsorption. So, the number of the active sites for methanol dissociation decreases effectively with increasing Pt loading for the Pt/TiO₂ catalysts reduced in H₂ at 400 °C. For the Pt/TiO₂ catalysts reduced in H₂ at 200 °C, the effects of SMSI almost do not occur [28] and the active sites for methanol adsorption do not decrease obviously with increasing Pt loading. Because the synergetic effect between the Pt and the surface active sites on TiO₂ is important for the H₂ generation reaction (reaction (1)) and the number of the released H⁺ correlates with the surface active sites on TiO₂ [20], the apparent rate constant of reaction (1) decreases more strongly with increasing Pt loading for Pt/TiO₂-400 catalysts than for Pt/TiO₂-200 catalysts.

Table II shows the activity of H₂ production on Pt/TiO₂ catalysts measured under steady-state irradiation conditions. It can be seen that the decay rate of the long-lived electrons obtained from time-resolved IR measurements qualitatively correlates well with the activity of H₂ production under steady-state irradiation conditions. These results indicate that the slow kinetics of the long-lived electrons is important for the photocat-

TABLE II The activity of H₂ production on Pt/TiO₂ photocatalysts

Sample	H ₂ evolution rate/($\mu\text{mol/h}$)
Pt/TiO ₂ -200 (0.1 wt%)	1590
Pt/TiO ₂ -400 (0.1 wt%)	1423
Pt/TiO ₂ -200 (1.0 wt%)	1273
Pt/TiO ₂ -400 (1.0 wt%)	990

alytic reaction of methanol for H₂ production. Though the photooxidation reaction of adsorbed methanol with the photogenerated holes proceeds ultrafast on picosecond time scale [19], the slow photoreduction reaction also directly influences the whole photocatalytic redox reaction. If the photogenerated electrons can't be consumed soon through reaction (1), the electrons will be accumulated in the catalyst and the whole photocatalytic redox reaction can't proceed well. On the contrary, if the electrons quickly take part in reaction (1), the whole photocatalytic reaction can proceed smoothly. Hence, the rate constant of reaction (1) that can be evaluated by time-resolved IR measurements is one of the considerable aspects in designing a photocatalyst with high activity for this photocatalytic reaction. On the basis of the results reported in this article, it is initially deduced that a Pt/TiO₂ catalyst (the supporter is the same) with suitable Pt loading amount and more surface active sites may have high activity for this photocatalytic reaction.

IV. CONCLUSION

Time-resolved IR spectroscopy was successfully used to detect the electron consuming reaction for H₂ generation on Pt/TiO₂ catalyst in the presence of methanol. There existed an optimal amount of Pt loading for the decays of the long-lived electrons in Pt/TiO₂-200 catalysts and the maximum decay rate was obtained for Pt/TiO₂ catalysts with 0.1 wt%Pt loading. The long-lived electrons in Pt/TiO₂-200 (0.1-1.0 wt%) catalysts decay faster than those in Pt/TiO₂-400 (0.1-1.0 wt%) catalysts when the Pt loading amount is the same. The decay rate of the long-lived electrons obtained from time-resolved IR measurements is one of the important parameters that determine the activity of H₂ production under steady-state irradiation conditions.

V. ACKNOWLEDGMENTS

The author Tao Chen is grateful to Professor Takaki Ishibashi and Mr. Kentaro Tanabe for their helpful discussions on time-resolved IR instrument. This work was supported by the National Natural Science Foundation of China (No.20373069 and No.20590363), the Knowledge Innovation Program of Chinese Academy

of Sciences, Dalian Institute of Chemical Physics (No.K2006E2) and the National Basic Research Program of China (No.2003CB615806, No.205CB221407, and No.2003CB214504).

- [1] J. Arana, J. M. Dona-Rodriguez, O. Gonzalez-Diaz, E. Tello Rendon, J. A. Herrera Melian, G. Colon, J. A. Navio, and J. Perez Pena, *J. Mol. Catal. A: Chem.* **215**, 153 (2004).
- [2] Z. Ding, G. Q. Lu, and P. F. Greenfield, *J. Phys. Chem. B* **104**, 4815 (2000).
- [3] A. Fujishima and K. Honda, *Nature* **238**, 37 (1972).
- [4] T. Sakata and T. Kawai, *Chem. Phys. Lett.* **80**, 341 (1981).
- [5] G. R. Bamwenda, S. Tsubota, T. Kobayashi, and M. Haruta, *J. Photochem. Photobiol. A: Chem.* **77**, 59 (1994).
- [6] B. O'Regan and M. Gratzel, *Nature* **353**, 737 (1991).
- [7] M. K. Nazeeruddin, A. Kay, I. Rodicio, R. Humphry-Baker, E. Muller, P. Liska, N. Vlachopoulos, and M. Gratzel, *J. Am. Chem. Soc.* **115**, 6382 (1993).
- [8] K. Iwata, T. Takaya, H. Hamaguchi, A. Yamakata, T. Ishibashi, H. Onishi, and H. Kuroda, *J. Phys. Chem. B* **108**, 20233 (2004).
- [9] G. Rothenberger, J. Moser, M. Gratzel, N. Serpone, and D. K. Sharma, *J. Am. Chem. Soc.* **107**, 8054 (1985).
- [10] A. Furube, T. Asahi, H. Masuhara, H. Yamashita, and M. Anpo, *J. Phys. Chem. B* **103**, 3120 (1999).
- [11] A. Furube, T. Asahi, H. Masuhara, H. Yamashita, and M. Anpo, *Chem. Phys. Lett.* **336**, 424 (2001).
- [12] S. H. Szczepankiewicz, J. A. Moss, and M. R. Hoffmann, *J. Phys. Chem. B* **106**, 2922 (2002).
- [13] A. Yamakata, T. Ishibashi, and H. Onishi, *J. Mol. Catal. A: Chem.* **199**, 85 (2003).
- [14] D. S. Warren and A. J. McQuillan, *J. Phys. Chem. B* **108**, 19373 (2004).
- [15] T. L. Thompson and J. T. Jr. Yates, *Chem. Rev.* **106**, 4428 (2006).
- [16] H. Zhao, Q. L. Zhang, and Y. X. Weng, *J. Phys. Chem. C* **111**, 3762 (2007).
- [17] A. Yamakata, T. Ishibashi, and H. Onishi, *J. Phys. Chem. B* **106**, 9122 (2002).
- [18] A. Yamakata, T. Ishibashi, and H. Onishi, *J. Phys. Chem. B* **107**, 9820 (2002).
- [19] Y. Tamaki, A. Furube, M. Murai, K. Hara, R. Katoh, and M. Tachiya, *J. Am. Chem. Soc.* **128**, 416 (2006).
- [20] T. Chen, Z. C. Feng, G. P. Wu, J. Y. Shi, G. J. Ma, P. L. Ying, and C. Li, *J. Phys. Chem. C* **111**, 8005 (2007).
- [21] Z. Lei, G. Ma, M. Liu, W. You, H. Yan, G. Wu, T. Takata, M. Hara, K. Domen, and C. Li, *J. Catal.* **237**, 322 (2006).
- [22] T. Berger, M. Sterrer, O. Diwald, E. Knozinger, D. Panayotov, T. L. Thompson, and J. T. Yates Jr., *J. Phys. Chem. B* **109**, 6061 (2005).
- [23] A. Yamakata, T. Ishibashi, and H. Onishi, *Chem. Phys. Lett.* **333**, 271 (2001).
- [24] L. C. Du and Y. X. Weng, *J. Phys. Chem. C* **111**, 4567 (2007).
- [25] Y. X. Weng, Y. Q. Wang, J. B. Asbury, H. N. Ghosh, and T. Q. Lian, *J. Phys. Chem. B* **104**, 93 (2000).
- [26] E. A. Taylor and G. L. Griffin, *J. Phys. Chem.* **92**, 477 (1988).
- [27] W. Wu, C. Chuang and J. Lin, *J. Phys. Chem. B* **104**, 8719 (2000).
- [28] S. J. Tauster, S. C. Fung, and R. L. Garten, *J. Am. Chem. Soc.* **100**, 170 (1978).
- [29] S. Tauster, *Acc. Chem. Res.* **20**, 379 (1987).